SCIENCE ADVANCES | RESEARCH ARTICLE

DISEASES AND DISORDERS

Neutrophil-mediated carbamylation promotes articular damage in rheumatoid arthritis

Liam J. O'Neil[1,2], Ana Barrera-Vargas[3], Donavon Sandoval-Heglund[1], Javier Merayo-Chalico[3], Eduardo Aguirre-Aguilar[3], Angel M. Aponte[4], Yanira Ruiz-Perdomo[5], Marjan Gucek[4], Hani El-Gabalawy[2], David A. Fox[6], James D. Katz[5], Mariana J. Kaplan[1]*, Carmelo Carmona-Rivera[1]*

Formation of autoantibodies to carbamylated proteins (anti-CarP) is considered detrimental in the prognosis of erosive rheumatoid arthritis (RA). The source of carbamylated antigens and the mechanisms by which anti-CarP antibodies promote bone erosion in RA remain unknown. Here, we find that neutrophil extracellular traps (NETs) externalize carbamylated proteins and that RA subjects develop autoantibodies against carbamylated NET (cNET) antigens that, in turn, correlate with levels of anti-CarP. Transgenic mice expressing the human RA shared epitope (HLADRB1* 04:01) immunized with cNETs develop antibodies to citrullinated and carbamylated proteins. Furthermore, anti–carbamylated histone antibodies correlate with radiographic bone erosion in RA subjects. Moreover, anti–carbamylated histone–immunoglobulin G immune complexes promote osteoclast differentiation and potentiate osteoclast-mediated matrix resorption. These results demonstrate that carbamylated proteins present in NETs enhance pathogenic immune responses and bone destruction, which may explain the association between anti-CarP and erosive arthritis in RA.

INTRODUCTION

Rheumatoid arthritis (RA) is an autoimmune condition that affects around 1% of the population worldwide. RA is characterized by inflammation of the synovial joints, cartilage damage, and periarticular bone erosions. Most RA patients develop autoantibodies against citrullinated proteins called ACPAs (*1*). Citrullination is a posttranslational modification where arginine is enzymatically converted to citrulline by peptidyl arginine deiminases (PADs) (*2*). ACPAs are highly specific to RA, and they can be detected years before the onset of clinical arthritis (*3*, *4*).

Recently, antibodies to another posttranslational modification called carbamylation have been described in RA subjects (*5*). Carbamylation is a nonenzymatic posttranslational modification that occurs primarily in lysine residues. Around 50% of RA subjects develop autoantibodies to carbamylated proteins (anti-CarP); the presence of these autoantibodies is associated with the development of a higher degree of bone erosions and with increased morbidity and mortality in RA patients (*5*–*7*). The exact source of carbamylated proteins that leads to the development of anti-CarP has yet to be determined. As previously described, carbamylation requires the presence of cyanate (CN^-), which may be generated enzymatically from thiocyanate (SCN^-) by myeloperoxidase (MPO) in sites of inflammation (*8*). Sources of thiocyanate may be derived from diet, but its presence is most commonly linked with cigarette smoking, a known risk factor for the development of RA. Smoking has been associated with anti-CarP production through its ability to increase carbamylation of vimentin in mice (*9*). Currently, anti-CarP antibodies are quantified using an enzyme-linked immunosorbent assay (ELISA) coated with fetal calf serum that has been exposed to high levels of CN^- (*5*). Despite its clear potential as a useful biomarker of poor prognosis in RA subjects, the source of individual carbamylated autoantigens remains elusive. Furthermore, whether carbamylation and the immune responses directed at carbamylated antigens play a pathogenic role in RA is unknown.

Neutrophils are highly abundant in the synovium of RA patients. We have shown that RA neutrophils display an enhanced capacity to form neutrophil extracellular traps (NETs) (*10*). NET formation leads to the externalization of citrullinated autoantigens that promote an adaptive immune response in which fibroblast-like synoviocytes (FLS) function as antigen-presenting cells (*11*). Here, we have investigated whether NETs represent a source of carbamylated autoantigens, whether RA subjects develop autoantibodies against carbamylated neoantigens present in NETs, and whether there is an association between autoantibodies and erosive joint disease. We also sought to establish the contribution of anti–carbamylated NET (cNET) protein antibodies in the differentiation and functional activity of osteoclasts (OCs), the cells responsible for bone erosion, as a mechanistic link between cNET autoantibody responses and bone damage.

RESULTS

Carbamylated protein–DNA complexes are elevated in RA plasma

Citrullinated histone H3–DNA complexes are putative markers of circulating NET remnants in circulation (*12*). Given that RA neutrophils display enhanced NET formation (*10*), we measured citrullinated histone H3–DNA complexes in plasma samples from healthy controls and two independent RA cohorts (table S1). Both RA cohorts displayed significant increases of citrullinated histone H3–DNA complexes when compared to healthy volunteers (Fig. 1A), supporting the previous observations of enhanced NET formation in RA. Because carbamylation is a posttranslational modification that has

[1]Systemic Autoimmunity Branch, National Institute of Arthritis and Musculoskeletal and Skin Diseases, National Institutes of Health, Bethesda, MD 20892, USA. [2]Manitoba Centre for Proteomics and Systems Biology, Department of Internal Medicine, University of Manitoba, Winnipeg, MB, Canada. [3]Department of Immunology and Rheumatology, Instituto Nacional de Ciencias Medicas y de la Nutricion, Salvador Zubiran, Mexico City, Mexico. [4]Proteomic Core, National Heart, Lung and Blood Institute, National Institutes of Health, Bethesda, MD 20892, USA. [5]Office of the Clinical Director, National Institute of Arthritis and Musculoskeletal and Skin Diseases, National Institutes of Health, Bethesda, MD 20892, USA. [6]Division of Rheumatology and Clinical Autoimmunity Center of Excellence, Department of Internal Medicine, University of Michigan, Ann Arbor, MI 48109, USA.
*Corresponding author. Email: carmelo.carmona-rivera@nih.gov (C.C.-R.); mariana.kaplan@nih.gov (M.J.K.)

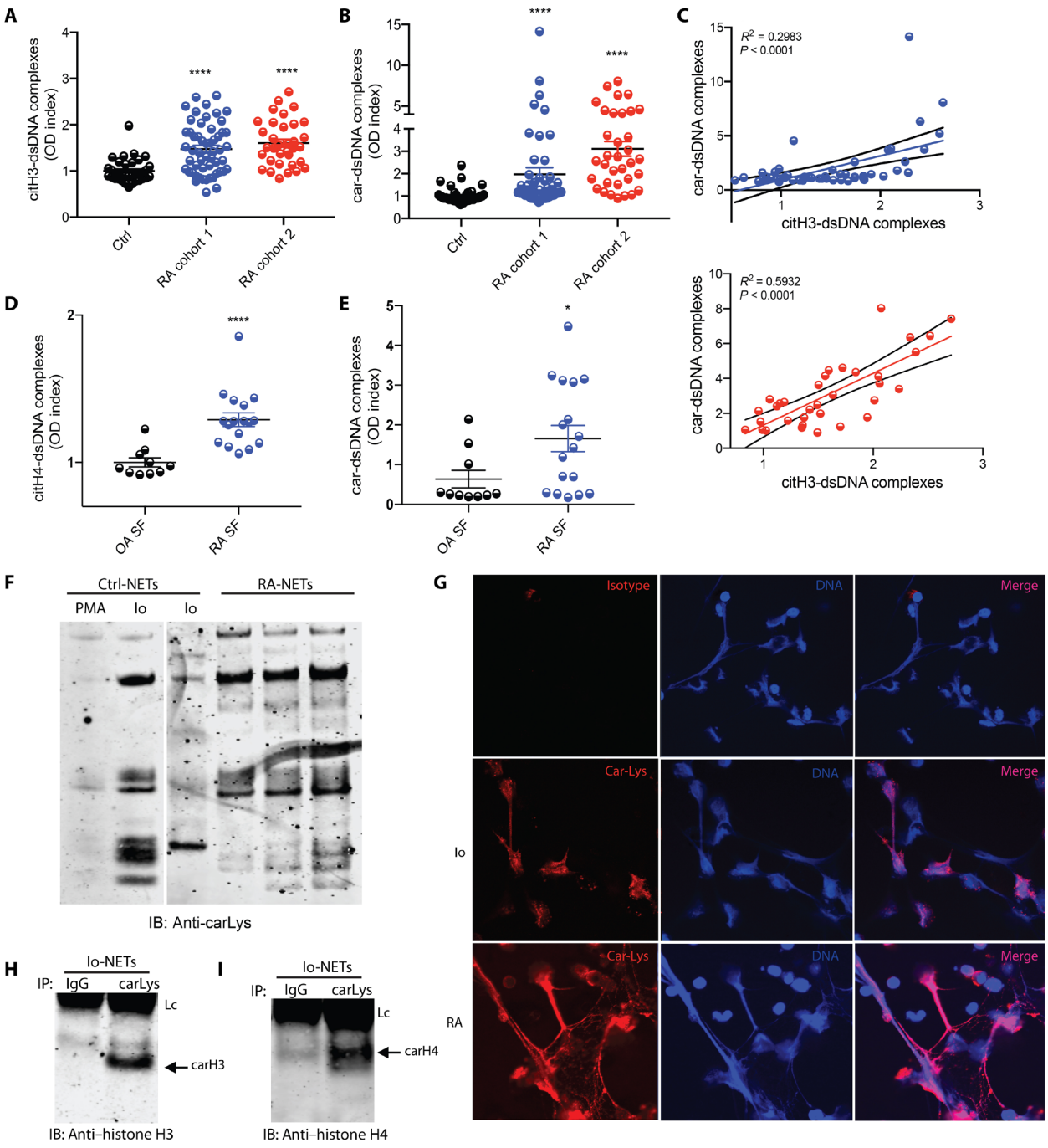

Fig. 1. Carbamylated proteins are increased in ionophore-generated NETs and in serum from RA subjects. (**A**) Citrullinated histone H3–dsDNA complexes were measured in plasma from healthy controls ($n = 25$), RA cohort 1 (blue, $n = 35$), and RA cohort 2 (red, $n = 34$). Results are the mean ± SEM. Kruskal-Wallis test was used. *$P < 0.05$ and ****$P < 0.0001$. (**B**) Carbamylated lysine–dsDNA complexes were measured in plasma from healthy control ($n = 25$), RA cohort 1 (blue, $n = 35$), and RA cohort 2 (red, $n = 34$) (**C**) Citrullinated histone H3 and DNA complexes correlate with carbamylated lysine–dsDNA complexes. (**D**) Citrullinated histone H3–dsDNA complexes were measured in SF from OA ($n = 10$) and RA ($n = 17$). Results are the mean ± SEM. Mann-Whitney *U* test was used. (**E**) Carbamylated lysine–dsDNA complexes were measured in SF from OA ($n = 10$) and RA ($n = 17$) patients. Results are the mean ± SEM. Mann-Whitney *U* test was used. (**F**) Western blot analysis of carbamylated proteins in PMA, ionophore (Io)–generated NETs, and spontaneously generated NETs from RA patients. Representative picture of three independent experiments. (**G**) Immunofluorescence detection of carbamylated proteins in ionophore-generated NETs. Representative picture of three independent experiments. Carbamylated proteins are in red; DNA is blue. Original magnification, ×400. Ionophore-generated NETs were immunoprecipitated (IP) using anti–carbamylated lysine antibody. Immunoblot (IB) analysis was performed against (**H**) histone H3 or (**I**) histone H4. IgG was used as negative control. Lc, light chain.

been implicated in RA pathogenesis, we investigated whether carbamylated protein–DNA complexes were also elevated in RA patients. We first tested and confirmed the specificity of the commercially available antibodies against citrullinated histone H3 and carbamylated lysine to discriminate between these two posttranslational modifications (fig. S1). Then, we developed an in-house sandwich ELISA to quantify plasma levels of carbamylated protein–DNA complexes in the same two RA cohorts as compared to healthy volunteers. Levels of these complexes were significantly increased in both RA cohorts (Fig. 1B). A positive correlation between levels of citrullinated histone H3–DNA complexes and carbamylated protein–DNA complexes suggested that the carbamylated complexes generate from NET structures (Fig. 1C). As RA synovial fluid (SF) neutrophils display an enhanced capacity to form NETs (*10*), we investigated whether carbamylated protein–DNA complexes were elevated in RA SF. Significantly increased levels of both citrullinated histone H3–DNA complexes (Fig. 1D) and carbamylated protein–DNA complexes (Fig. 1E) were detected in RA SF when compared to SF obtained from subjects with osteoarthritis (OA). To further corroborate that carbamylated proteins can be found in NETs, healthy control neutrophils were stimulated with phorbol 12-myristate 13-acetate (PMA) or calcium ionophore A23187 for 4 hours to induce NET formation, per methods previously described (*13*, *14*). NETs were purified and probed against carbamylated lysine by Western blot. Multiple carbamylated proteins were detected in spontaneously generated NETs from RA neutrophils or NETs induced by calcium ionophore in healthy control neutrophils, but not in NETs induced with PMA in healthy control neutrophils (Fig. 1F). Immunofluorescence analysis corroborated the presence of carbamylated proteins in ionophore-generated NETs from healthy control neutrophils and in spontaneously generated NETs from RA neutrophils (Fig. 1G). Immunoprecipitation studies demonstrated that histones H3 and H4 are carbamylated in ionophore-generated NETs (Fig. 1, H and I). To further corroborate that histones H3 and H4 were carbamylated in ionophore-generated NETs, mass spectrometry analysis was performed. We found that eight lysine residues were carbamylated in histone H3, while five sites were carbamylated in histone H4 (Table 1). These findings support the notion that NETs are a source of carbamylated autoantigens in RA.

Table 1. Identified sites of carbamylation. Proteomic analysis was performed on ionophore-generated NETs according to Materials and Methods. Underlined k's (red) are carbamylated lysines.

Protein	Peptide sequence	Modification name	Position(s) in protein
Histone H3	kQLATkAAR	Carbamyl	19, 24
	kSAPATGGVkkPHR	Carbamyl	28, 37, 38
	YQkSTELLIR	Carbamyl	57
	EIAQDFkTDLR	Carbamyl	80
	VTIMPkDIQLAR	Carbamyl	123
Histone H4	kVLRDNIQGITkPAIR	Carbamyl	21, 32
	DNIQGITkPAIR	Carbamyl	32
	DAVTYTEHAkR	Carbamyl	78
	kTVTAMDVVYALkR	Carbamyl	80, 92

RA patients develop autoantibodies against cNET proteins

To further study the role of carbamylation in RA, we generated both NETs with low to absent carbamylation and NETs containing high amounts of carbamylated proteins. PMA-generated NETs displayed the lowest amount of carbamylation when compared to calcium ionophore–induced NETs (Fig. 1F). To increase the degree of carbamylation, we incubated control neutrophils in the presence of both PMA and cyanate (CN). Western blot analysis of purified NETs generated in the presence of CN demonstrated increased carbamylation when compared to PMA alone (Fig. 2A). Immunofluorescence analysis showed that purified RA IgGs (immunoglobulin Gs) and ACPA-depleted RA-IgG bind to these highly carbamylated NETs, whereas isolated IgGs from control sera did not (Fig. 2B). To further corroborate this observation, the ability of RA serum to bind to highly carbamylated NETs was tested by ELISA. Serum samples from two RA cohorts displayed significantly enhanced reactivity to cNETs when compared to serum from healthy volunteers (Fig. 2C). These results suggest that autoantibodies against cNET proteins are generated in RA patients.

Given that histones are carbamylated in NETs (Fig. 1, H and I) and that vimentin and α-enolase have been reported to be important autoantigens in RA as well as to be present in NETs (*10*), we tested whether RA patients develop autoantibodies against carbamylated versions of these proteins. Recombinant proteins were carbamylated in vitro in the presence of 100 μM CN overnight. Western blot analysis confirmed that carbamylation of each antigen was generated. Plates were coated with each carbamylated antigen, and the presence of antibodies against the carbamylated forms of these proteins was assessed in healthy control, RA, and systemic lupus erythematosus (SLE) serum samples. RA patients displayed significantly higher titers of antibodies directed against carbamylated forms of histones H2A (Fig. 2D), H3 (Fig. 2E), H4 (Fig. 2F), and H2B (Fig. 2G) and of vimentin (Fig. 2H) when compared to healthy volunteers. The specificity of the carbamylated antibodies present in RA patients was tested in ACPA-depleted sera (fig. S2, A to E). Moreover, purified ACPAs from RA patients displayed minimal to no cross-reactivity to the carbamylated version of histone H3, histone H4, and vimentin, as shown by Western blot analysis (fig. S3, A to C). Antibodies against carbamylated elastase and α-enolase [both proteins present in NETs (*15*)] were also elevated in RA samples (fig. S4, A and B). Moreover, most of these antibodies were specifically elevated in RA subjects but not in samples from SLE subjects, with the exception of anti–carbamylated histone H2A (Fig. 2D). Longitudinal analysis confirmed that anti–carbamylated histone antibodies were significantly elevated in RA patients at various time points of the follow-up (fig. S5, A to C).

Approximately 35 to 50% of RA subjects develop antibodies against carbamylated fetal bovine serum (FBS) (anti-CarP antibodies) (*5*, *16*, *17*), but the specific carbamylated antigens and their source remain unclear. We found that anti-CarP antibodies were significantly elevated in the two RA cohorts tested in this study, when compared to healthy volunteers (Fig. 3A). To gain insight concerning the relevance of antibodies toward cNET proteins found in RA subjects, correlation analyses were performed, demonstrating that anti-CarP antibodies significantly correlate with the levels of anti–carbamylated histone H3 (Fig. 3B), anti–carbamylated H2B (Fig. 3C), anti–carbamylated histone H4 (Fig. 3D), anti–carbamylated vimentin (Fig. 3E), and anti–carbamylated α-enolase (Fig. 3F). Furthermore, anti-CarP antibodies significantly correlated with the levels of anti–carbamylated

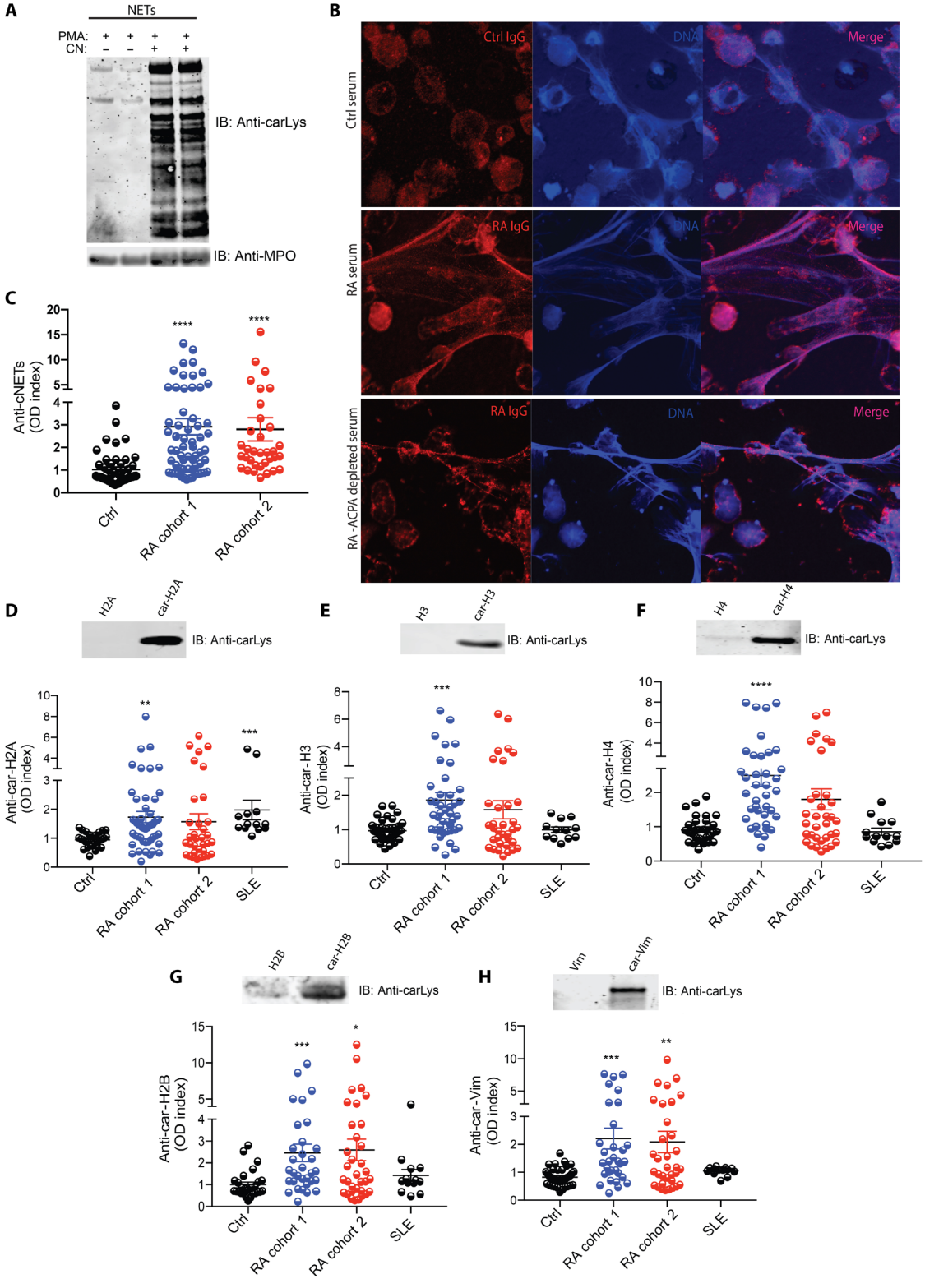

Fig. 2. Autoantibodies against cNET proteins are present in serum from RA patients. (**A**) Western blot analysis shows increased cNET proteins after incubation with CN. RA IgGs recognize highly carbamylated (CN + PMA) NETs by (**B**) immunofluorescence and (**C**) ELISA analysis. Red, RA IgG; blue, DNA. Results are the mean ± SEM. Kruskal-Wallis test was used. Sera from healthy control ($n = 25$), RA cohort 1 (blue, $n = 35$), RA cohort 2 (red, $n = 34$), and SLE ($n = 12$) were analyzed for the presence of antibodies against carbamylated histones (**D**) H2A, (**E**) H3, (**F**) H4, and (**G**) H2B and against (**H**) vimentin. Results are the mean ± SEM. Kruskal-Wallis test was used. *$P < 0.05$, **$P < 0.01$, ***$P < 0.001$, and ****$P < 0.0001$. Western blot analysis was used to confirm carbamylation of each antigen [top panels of (D) to (H)]. Original magnification, ×400.

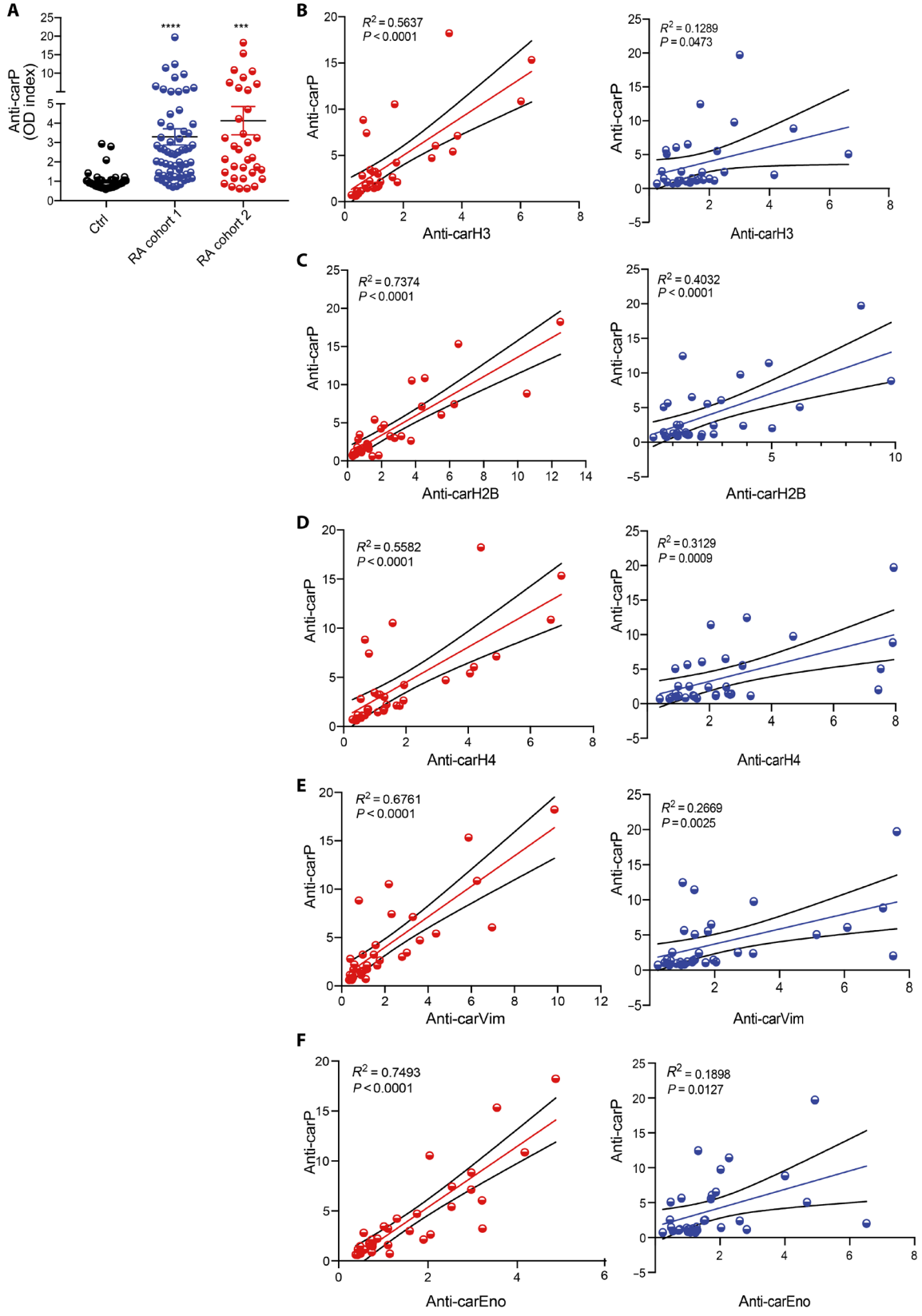

Fig. 3. Autoantibodies against cNET antigens correlate with anti-CarP antibodies. (**A**) Serum anti-CarP levels were measured in healthy control ($n = 25$), RA cohort 1 (blue, $n = 35$), and RA cohort 2 (red, $n = 34$). Results are the mean ± SEM. Kruskal-Wallis test was used. ***$P < 0.001$ and ****$P < 0.0001$. Correlation of anti-CarP antibodies with antibodies against carbamylated (**B**) histone H3, (**C**) histone H2B, (**D**) histone H4, (**E**) vimentin, and (**F**) α-enolase in two RA cohorts (red and blue).

neutrophil elastase (fig. S6A) and anti–carbamylated histone H2A (fig. S6B) in RA cohort 2 (shown in red) but not in RA cohort 1 (shown in blue) (fig. S6, A and B). These results suggest that RA patients positive for anti-CarP develop autoantibodies against cNET proteins and that NETs are a source of carbamylated neoantigens.

HLA-DRB1*04:01 transgenic mice develop anti-CarP and ACPAs in response to immunization with cNETs

To confirm that NETs are a source of carbamylated proteins and that they can induce adaptive immune responses toward carbamylated proteins in vivo, we used the humanized HLA-DRB1*04:01 transgenic mouse model. These animals lack the endogenous class II molecule and instead express the DR1 allele that confers susceptibility to inflammatory arthritis by immunization with various stimuli (*18*–*20*). PMA-generated NETs were isolated from peripheral blood (PB) control neutrophils in the presence or absence of CN. The presence of carbamylated proteins in these NETs was confirmed by Western blot (Fig. 4A), while the presence of citrullination was assessed using a rhodamine phenylglyoxal (Rh-PG)–based probe (Fig. 4B). Differences in citrullination and carbamylation patterns were evident in these NETs. PMA-generated NETs have been reported to have low amounts of citrullination (*13*). In contrast, we found that PMA-generated NETs in the presence of CN displayed increased citrullination when compared to PMA-generated NETs in the absence of CN (Fig. 4B). The levels of citrullinated histone H3 were significantly elevated in NETs generated in the presence of PMA and CN when compared to those generated with just PMA (Fig. 4, B and C). Mice underwent 12 weekly injections of cNETs, at which

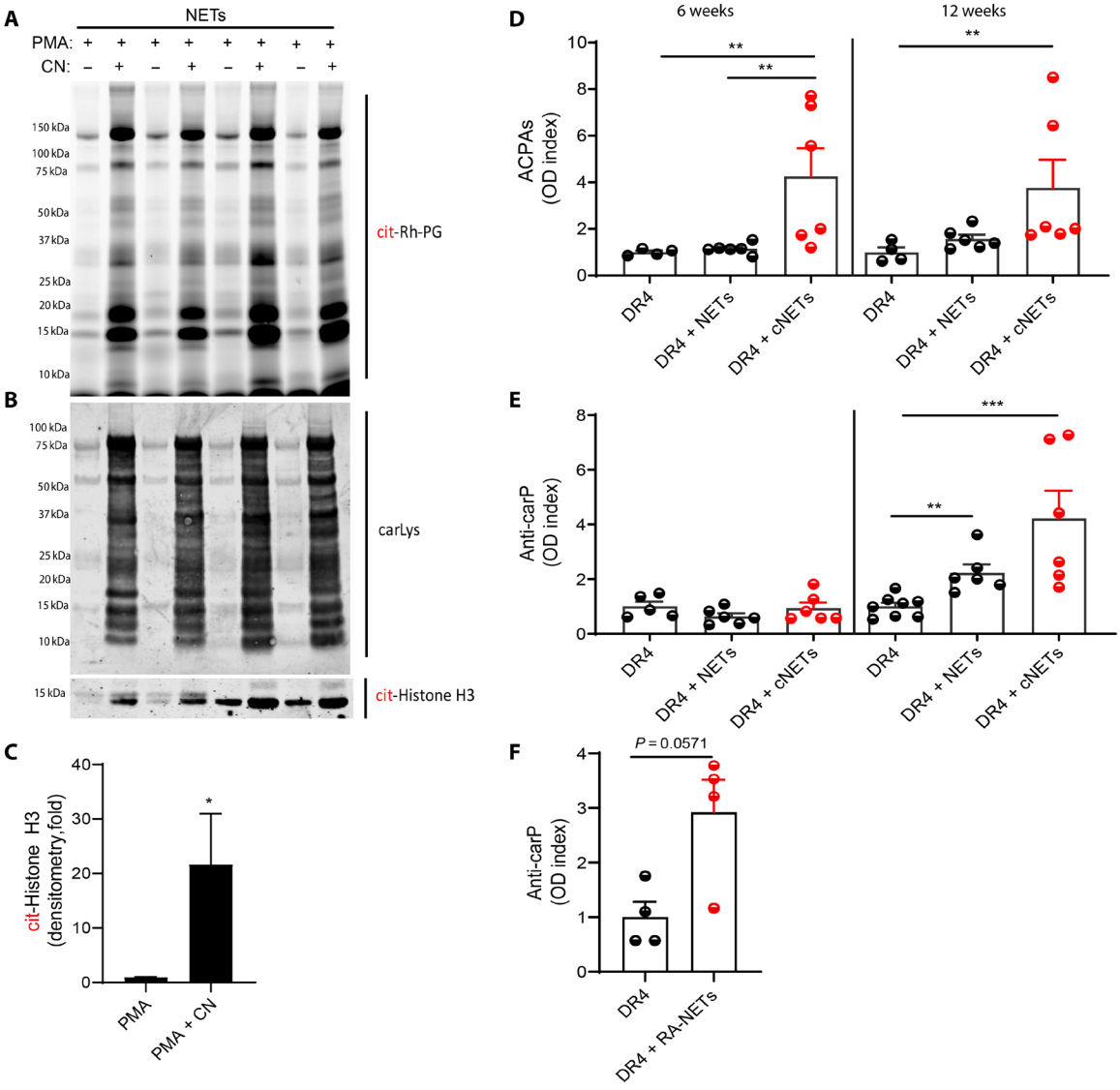

Fig. 4. DRB1*04:01 (DR4) transgenic mice that receive intra-articular injections of cNETs develop ACPAs and anti-CarP. (**A**) Rh-PG probe against citrulline was used to detect specific citrullinated proteins in NETs (PMA) and cNETs (PMA + CN). (**B**) Western blot analysis against carbamylated proteins was performed in NET and cNETs. (**C**) Densitometry analysis of citrullinated histone H3 in NETs generated with PMA or PMA + CN ($n = 4$ per group). Results are the mean ± SEM. Mann-Whitney *U* test was used. *$P < 0.05$. (**D**) Serum ACPAs and (**E** and **F**) anti-CarP antibody levels were measured at various points in animals immunized with NETs, cNETs, or spontaneously generated RA-NETs ($n = 4$ to 8 per group). Results are the mean ± SEM. Kruskal-Wallis test was used. **$P < 0.01$ and ***$P < 0.001$.

point serum ACPAs and anti-CarP levels were quantified. Significantly higher titers of ACPAs were detected in sera of mice that received intra-articular injections of cNETs, at weeks 6 and 12, when compared with animals that received PMA-generated NETs (Fig. 4D). This may be explained by the observation that cNETs contain higher amounts of citrullinated proteins, when compared to PMA-generated NETs (Fig. 4, B and C). Of note, the kinetics of autoantibody development in vivo, in response to cNETs, differed for anti-CarP and ACPAs. Anti-CarP antibodies were detected by week 12 of immunization, but not at week 6, while ACPAs were already detected by week 6 and continued to be detected at week 12 (Fig. 4E). In addition, animals that received spontaneously generated RA NETs developed significantly increased titers of anti-CarP antibodies when compared to controls, supporting the hypothesis that NETs are a source of carbamylated antigens that can stimulate anti-CarP responses (Fig. 4F). These results indicate a sequential generation of antibodies, where response to citrullinated peptides precedes the responses to carbamylated peptides. Overall, these results demonstrate that highly carbamylated NETs can induce an adaptive immune response toward cNETs in vivo.

Antibodies to carbamylated histones correlate with degree of bone erosions in RA

To investigate the clinical relevance of anti-cNET protein antibodies in RA patients, correlation analyses were performed. Smoking has been associated with carbamylation and/or the presence of anti-CarP because it is a source of thiocyanate that can be transformed into CN (*7*). However, we did not find a significant correlation between smoking and the presence of carbamylated protein–DNA complexes or autoantibodies against cNET proteins. Similarly, we did not observe a correlation with radiologic evidence of bone erosion (Fig. 5). Significant correlations were found between carbamylated protein–DNA complexes and levels of antibodies against carbamylated histone H3 ($P = 0.042$), histone H4 ($P = 0.038$), histone H2A, ($P = 0.043$), vimentin ($P = 0.011$), α-enolase ($P = 0.036$), anti-CarP ($P = 0.032$), and rheumatoid factor (RF) ($P = 0.024$) (Fig. 5), suggesting that subjects with elevated carbamylated protein–DNA complexes also develop autoantibodies against cNET components. Levels of citrullinated histone H3–DNA complexes (characteristic of NET remnants in circulation) significantly correlated with anti–carbamylated vimentin ($P = 0.048$) and anti-CarP antibodies ($P = 0.044$) (Fig. 5). The presence of anti–carbamylated H2A positively correlated with global health ($P = 0.030$) and with the disease activity score in 28 joints–erythrocyte sedimentation rate (DAS28-ESR) score, an assessment of joint inflammation in RA ($P = 0.042$) (Fig. 5). Anti–carbamylated vimentin antibodies also correlated with DAS28 ($P = 0.042$). The presence of periarticular bone erosions in the hands significantly correlated with the presence of anti–carbamylated histone H3 ($P = 0.025$), anti–carbamylated histone H4 ($P = 0.020$), anti–carbamylated H2A ($P = 0.012$), anti–carbamylated H2B ($P = 0.011$), anti–carbamylated vimentin ($P = 0.008$), anti–carbamylated α-enolase ($P = 0.008$), and anti-CarP ($P = 0.008$) antibodies (Fig. 5). Furthermore, anti–carbamylated histone H2B ($P = 0.011$), vimentin ($P = 0.032$), α-enolase ($P = 0.001$), and anti-CarP ($P = 0.028$) antibodies correlated with periarticular foot erosions

Fig. 5. Autoantibodies against carbamylated histones correlate with bone erosion. Visual representation of significant correlations of autoantibodies against cNET proteins, carbamylated protein–DNA complexes, anti-CarP, ACPAs, and rheumatoid factor (RF) measured in RA subjects with clinical outcomes ($n = 34$) (global health, smoking, DAS28-ESR, hand and feet erosion score). Color gradient represents R^2 values.

(Fig. 5). Moreover, the levels of anti–carbamylated histone H3 (β = 1.5; $P = 0.03$), histone H4 (β = 1.39; $P = 0.02$), and histone H2A (β = 1.5; $P = 0.03$) antibodies and ACPAs (β = 0.02; $P = 0.03$) correlated with radiologic hand erosion scores, while anti–carbamylated histone H3 (β = 0.48; $P = 0.010$), histone H4 (β = 0.46; $P = 0.006$), histone H2A (β = 0.53; $P = 0.004$), vimentin (β = 0.34; $P = 0.012$), enolase (β = 0.71; $P = 0.004$), and anti-CarP (β = 0.14; $P = 0.040$) antibodies correlated with foot erosion scores. These results suggest that anti–carbamylated autoantibodies may affect bone health and may predict intra-articular bone damage in RA.

cNETs activate FLS and macrophages and lead to OC differentiation

Macrophages and FLS play important roles in RA pathogenesis (*21*). We previously showed that NETs from RA subjects activate FLS (*10*, *11*). To expand our understanding of the effect of cNETs in the joint, we incubated macrophages and FLS in the presence or absence of PMA-generated NETs or cNETs for 24 hours. cNETs induced macrophages to significantly up-regulate proinflammatory cytokine genes, such as *tumor necrosis factor* (*TNF*), *interleukin-8* (*IL-8*), and *IL-6* when compared to untreated conditions or to PMA-generated NETs (fig. S7, A to C). By confocal microscopy, we found that NETs and cNETs are internalized by RA FLS (Fig. 6A). In addition, significant up-regulation of matrix metalloproteinase 1 (MMP1) and MMP3 mRNAs was evident after incubation with cNETs or spontaneously generated RA-NETs when compared to untreated RA FLS (Fig. 6, B and C, and fig. S8). In contrast, non-cNETs induced higher levels of IL-8 by RA FLS than cNETs (Fig. 6, D and E). cNETs also significantly up-regulated RANKL mRNA expression in RA FLS when compared to untreated cells (Fig. 6F). This was confirmed by flow cytometry, as the RANKL geometric mean of RA FLS cells treated with cNETs was significantly higher than untreated RA FLS (Fig. 6G). Because RANKL has the ability to stimulate OC formation (*22*, *23*), we hypothesized that the supernatants of RA FLS stimulated with cNETs would promote OC formation. To test this hypothesis, PB $CD14^+$ monocytes isolated from healthy volunteers were incubated in the presence or absence of supernatants of FLS stimulated with either NETs or cNETs. After 7 days of incubation, cells were stained for the presence of tartrate-resistant acid phosphatase (TRAP), a specific OC marker. Multinucleated, TRAP-positive cells were evident after incubation with supernatant from FLS stimulated with cNETs when compared to those from FLS stimulated with NETs (Fig. 6H). Of note, monocytes incubated with supernatants from FLS without NETs did not survive. These results suggest that cNETs up-regulate pathways in FLS that are involved in bone damage and OC formation/activation, in particular RANKL. In addition, interactions between FLS and cNET proteins promote the formation of OCs, a phenomenon conducive to joint erosions and bone damage.

Immune complexes of carbamylated histones enhance OC formation and activity

Anti-CarP has been associated with increased bone erosions in RA patients (*5*, *24*). Because we found that anti–carbamylated histone antibodies correlate with bone erosion scores (Fig. 5), we sought to determine if anti–carbamylated histone antibodies directly affect OC formation and resorption. Healthy volunteer PB $CD14^+$ monocytes were incubated with monocyte colony-stimulating factor (M-CSF)/RANKL in the presence or absence of carbamylated histone 3 and carbamylated histone 4 immune complexes. OC differentiation was significantly enhanced in the presence of anti–carbamylated histone H3/H4–RA–IgG immune complexes, when compared to carbamylated histone H3/H4 and carbamylated histone H3/H4 with control IgGs and OCs in the absence of immune complexes (Fig. 7, A and B). These results indicate that anti–carbamylated histone H3/H4 immune complexes accelerate OC formation. Equal numbers of OCs generated with M-CSF/RANKL were seeded on a calcium phosphate plate in the presence or absence of carbamylated histone H3/H4, carbamylated histone H3/H4 with control IgGs, or carbamylated histone H3/H4–RA–IgG immune complexes. RANKL was added to all conditions to activate OCs. Eroded surfaces were imaged using Celigo and quantified with ImageJ. Carbamylated histone H3/H4–RA–IgG immune complexes significantly enhanced OC resorptive activity when compared to OC without immune complexes (Fig. 7, C and D). These results suggest that anti–carbamylated histone H3/H4–RA–IgG immune complexes potentiate OC formation and activity, which may affect bone destruction.

DISCUSSION

Emerging evidence implicates neutrophils, particularly through NET formation, as important players in the generation of modified autoantigens in the RA synovium (*10*, *11*). Previous observations focused on the generation of citrullinated autoantigens and the induction of pathogenic anti-citrulline responses. Here, we show that NETs contain carbamylated autoantigens that can also promote pathogenic adaptive immunity, leading to generation of anti-CarP and anti-cNET protein antibodies. Furthermore, these cNETs can activate macrophages to synthesize proinflammatory cytokines and FLS to release RANKL that, in turn, promotes OC formation and activation. In addition, anti–carbamylated histone antibodies can form immune complexes that further potentiate OC formation and bone resorption, a phenomenon crucial in joint destruction in RA (Fig. 8).

In this study, we uncovered multiple NET-specific carbamylated autoantigens potentially important in RA. These carbamylated autoantibodies likely contribute to the autoreactivity measured by anti-CarP ELISAs in the early descriptions of this type of autoantibody. We provide a compelling mechanism that links anti-CarP and enhanced bone erosion in RA through the identification of the source of carbamylated antigens and their influence on pathogenic bone degradation.

RA synovial joints are characterized by hyperplasia of the synovial lining, which is composed of invasive FLS and an infiltration of immune cells such as neutrophils, T cells, macrophages, B cells, and plasma cells (*25*, *26*). Neutrophils are the most abundant cell type found in the SF of RA patients, and we have shown that the RA synovial microenvironment is highly conducive to the formation of NETs (*10*). During NET formation, citrullinated and carbamylated autoantigens are externalized to the extracellular space. FLS have the ability to acquire nonprofessional antigen-presenting cell capabilities in the RA synovial environment by internalizing NETs containing citrullinated autoantigens, up-regulating major histocompatibility complex (MHC) class II, and presenting the modified autoantigens to $CD4^+$ T cells in the context of the shared epitope (SE) (*11*). We now show that cNETs are also internalized by FLS, suggesting that a similar mechanism may mediate the breach in immune tolerance to carbamylated proteins.

Anti-CarP antibodies are emerging as a biomarker in RA because they associate significantly with destructive joint disease and poor

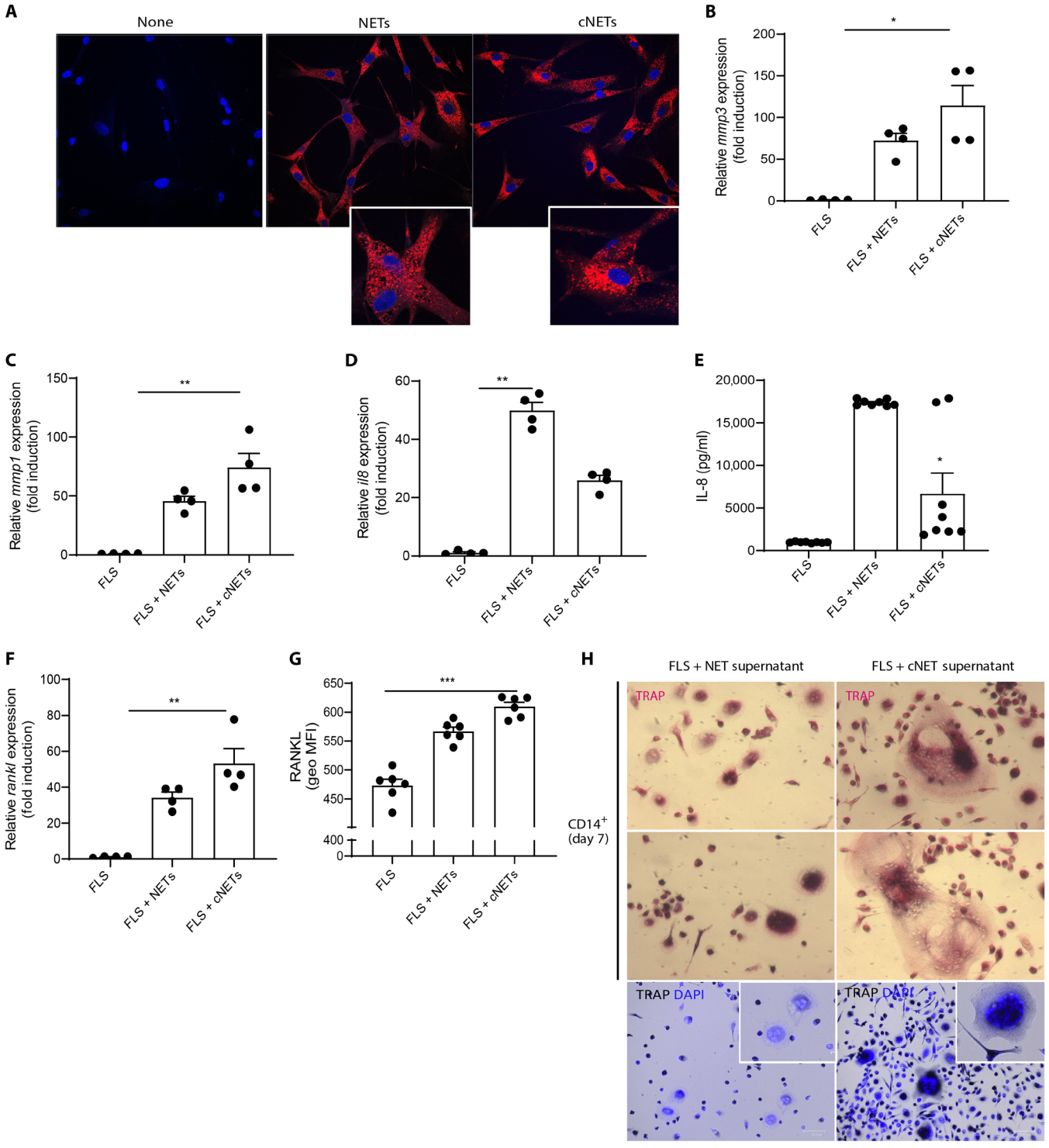

Fig. 6. cNETs up-regulate RANKL in FLS and promote OC formation. NETs and cNETs were incubated with RA FLS for 24 hours. (**A**) NETs and cNETs were internalized by RA FLS. Red, MPO; blue, DNA. Results are representative of three independent experiments. Original magnification, ×400. Quantitative polymerase chain reaction (qPCR) analysis shows (**B**) *MMP3*, (**C**) *MMP1*, (**D**) *IL8*, and (**F**) *RANKL* mRNA expression and ELISA analysis of (**E**) IL8 in RA FLS in the presence of NET and cNETs. Results are the mean ± SEM of four to eight independent experiments. Kruskal-Wallis test was used. *$P < 0.05$, **$P < 0.01$, and ***$P < 0.001$. (**G**) Plasma membrane RANKL was quantified by flow cytometry in RA FLS treated with NETs or cNETs for 24 hours. MFI, median fluorescent intensity. (**H**) $CD14^+$ monocytes were incubated with supernatants of RA FLS treated with NETs or cNETs for 7 days. The presence of OCs was defined as multinucleated, TRAP (magenta, black for lower panel)–positive cells; nuclei are in blue (lower panel). Results are representative of three independent experiments. Original magnification, ×400 and ×200 (lower panels).

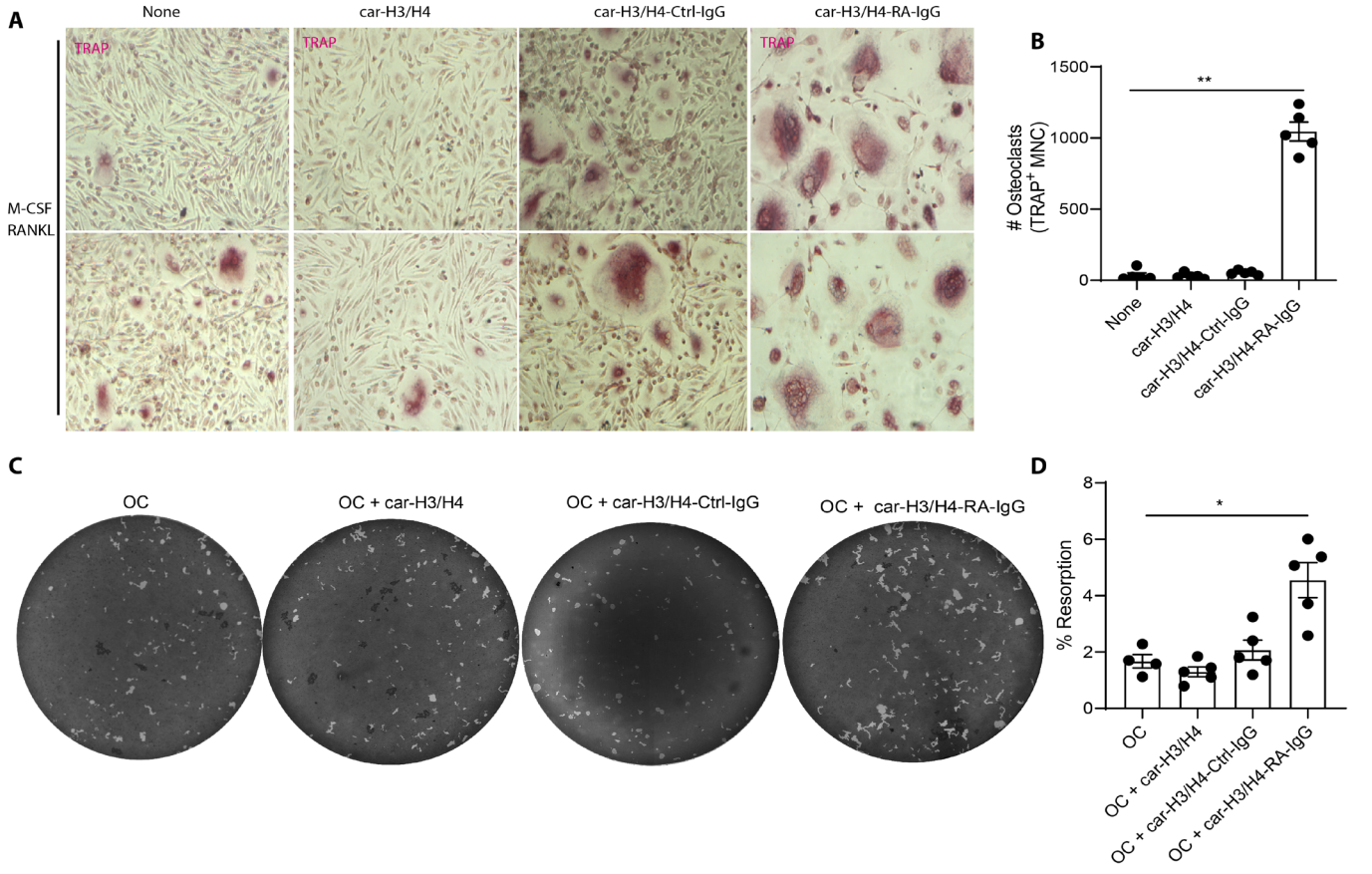

Fig. 7. Anti–carbamylated histone H3 and H4–IgG complexes increase osteoclastogenesis and bone matrix resorption. (**A**) Representative pictures of M-CSF/RANKL–mediated osteoclastogenesis in the presence or absence of anti–carbamylated histone H3/H4–IgG immune complexes. Original magnification, ×400. (**B**) Quantification of TRAP-positive multinucleated cells (MNC). Results are the mean ± SEM of four to five independent experiments. Kruskal-Wallis test was used. $^{**}P < 0.01$. (**C**) Representative pictures of resorption pit assay of equal number of M-CSF/RANKL–generated OCs in the presence or absence of anti–carbamylated histone H3/H4-IgG immune complexes in a calcium phosphate plate. (**D**) Percentage of eroded surface using ImageJ. Results are the mean ± SEM of four to five independent experiments. Mann-Whitney *U* test was used. $^{*}P < 0.05$.

patient outcomes (*5*, *6*, *24*). Little is known regarding the specific carbamylated autoantigens that drive anti-CarP formation in RA patients. We provide evidence that anti–carbamylated histones significantly associate with anti-CarP antibodies and, further, that they provide stronger association with bone erosion than anti-CarP or ACPAs. Consistent with other studies, ACPAs appear to cross-react with carbamylated proteins. Despite this, we provide evidence of persistent autoantibody reactivity to carbamylated antigens following ACPA depletion, supporting specific anti-CarP responses. Anti–carbamylated histones directly promote enhanced OC differentiation. Furthermore, mature OCs appear to be influenced by carbamylated histone immune complexes by augmenting bone resorption. Although the direct evidence that we provide between autoantibodies and bone loss may not be the only mechanism to explain the more severe phenotype for anti-CarP–positive patients, it represents an attractive link between anti-carbamylated antibodies and destructive joint disease. The principle that autoantibodies modify bone has been shown in cases of autoantibodies against citrullinated vimentin (*27*) and decoy receptor of RANKL (*28*) causing bone loss in RA and celiac disease, respectively. Furthermore, our data may also contribute to explaining the link between osteoporosis and anti-CarP in RA (*29*). Before our study, the role of carbamylation or autoantibodies against carbamylated proteins in bone homeostasis had been largely unexplored. Our findings reinforce a body of work implicating the adaptive immune system in promoting the induction of deleterious pathways leading to bone destruction. These results support the use of anti–carbamylated histones as an attractive biomarker for erosive and more aggressive disease (*30*, *31*).

Although we observed similar results between our two RA cohorts, the magnitude of association between anti-CarP and anti-cNET antigens was stronger in cohort 2. Some differences in a variety of baseline demographic characteristics were apparent between these cohorts (table S1); in particular, smoking prevalence was higher in cohort 2 compared to cohort 1. It remains possible that cigarette smoke exposure is one of the reasons for these observed differences, although testing this hypothesis will require analysis of larger sample sizes. Smoking is considered to be an important risk factor for the development of RA (*32*). One of the proposed mechanisms is that tobacco smoke increases citrullination of proteins present in the lungs (*33*). Another proposed mechanism is that cigarette smoke increases carbamylation of vimentin, as was shown in a mouse model (*9*). Cigarette smoke is a source of SCN^-, the precursor to CN^-, which mediates carbamylation in a variety of clinically relevant settings (*7*). Despite these reports, we did not find any correlation between

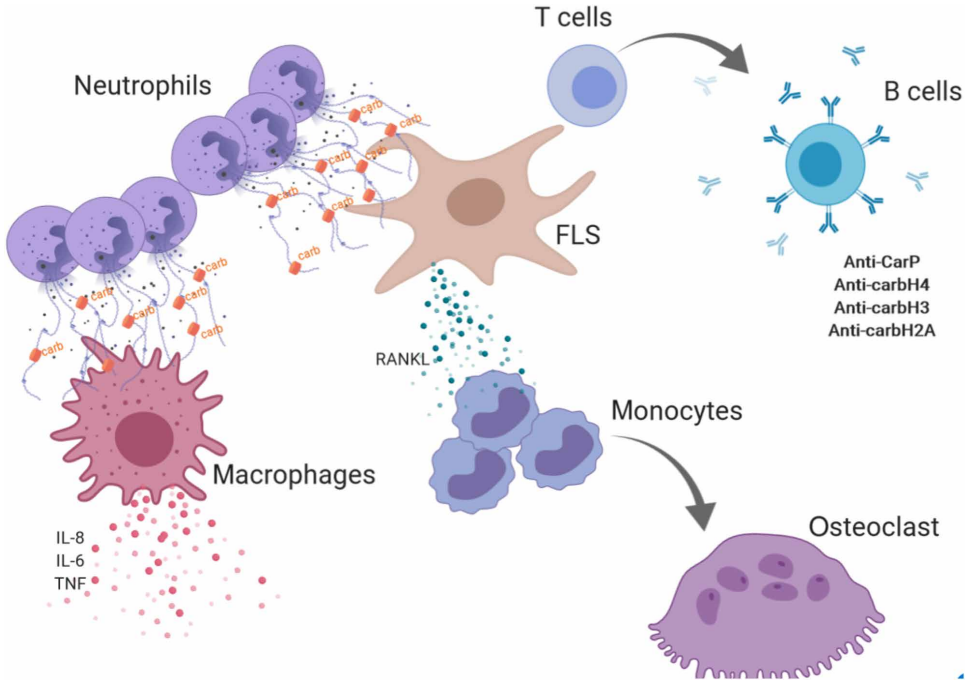

Fig. 8. Schematic representation of the role of carbamylation and anti-carbamylated immune responses in joint destruction in RA. Infiltrating neutrophils release NETs containing carbamylated proteins. cNETs activate tissue macrophages to release proinflammatory cytokines. cNETs are internalized by FLS and up-regulate FLS production of RANKL that promotes osteoclastogenesis in $CD14^+$ monocytes. Internalized cNETs by FLS can promote an adaptive immune response leading to generation of anti–carbamylated histone antibodies. In turn, these antibodies can form carbamylated immune complexes that promote OC formation and increase bone resorption.

autoantibodies against cNET proteins with current or past smoking. This lack of correlation may suggest that mechanisms other than tobacco smoke can also promote citrullination and carbamylation in RA subjects. We showed that calcium ionophore and spontaneous RA NET formation triggers carbamylation of relevant autoantigens, without the need for exogenous thiocyanate or CN. A previous report highlights a mechanism by which interaction between mitochondrial carbamoyl phosphate synthase-1 (CPS1) and aryl hydrocarbon receptor (AhR) results in translocation of the CPS1-AhR complex into the nucleus, leading to carbamylation of histone H1 and upregulation of PAD2, which, in turn, increases citrullination, suggesting a mechanism that could independently enhance both carbamylation and citrullination of intracellular proteins (*34*). This opens the door to consider other endogenous sources of the molecules that promote carbamylation in the RA joint. We also found that exogenous CN increases NET citrullination, suggesting that CN could have a role in activating PAD enzymes. This possibility should be explored in future studies.

Together, these data implicate neutrophils as a source of both citrullinated and carbamylated autoantigens in RA. We do not exclude other additional cell death mechanisms (such as necrosis, apoptosis, or pyroptosis) that could also promote externalization of carbamylated autoantigens. Common to many RA patients, the so-called SE predisposes carriers to the development of ACPA by efficiently presenting these antigens on MHC class II (*35*). Our study shows that HLA-DRB1*04:01 transgenic mice immunized with NETs containing citrullinated and carbamylated proteins displayed differential kinetics in the development of ACPAs and anti-CarP. These findings also support the notion that genetic susceptibility and environmental factors lead to generation of antibodies against posttranslational modified neoantigens. Although the role of the HLA-DRB1*04:01/04–positive allele has not been well established for anti-CarP antibodies, anti-CarP has been described in patients with the SE in the context of preclinical RA (*17*). Whether ACPA precedes the development of anti-CarP in RA patients remains to be determined. Despite this, we present evidence supporting the role of NETs for generation of both ACPA and anti-CarP in patients with the SE. Further investigation will be needed to corroborate these findings and support these hypotheses.

In summary, our observations highlight a previously unknown mechanism that connects neutrophil-mediated carbamylation, immune dysregulation, and bone erosion in RA. Our data extend the current understanding of the role of anti-CarP in bone erosion and provide evidence of previously unreported carbamylated autoantibodies that may serve as better predictor of bone and joint damage in RA patients. Thus, these findings provide a link between the generation of cNETs in the synovium and bone loss, and further support the use of these novel carbamylated autoantibodies as biomarkers for bone erosion in RA patients.

MATERIALS AND METHODS

Human specimens and cells

Subjects recruited in this study fulfilled the ACR (American College of Rheumatology) criteria for RA (*36*) or were diagnosed with OA based on characteristic clinical and radiographic features, and confirmed by pathological findings at joint surgery. Healthy controls were recruited by advertisement. SLE patients fulfilled the ACR revised diagnostic criteria (*37*). All individuals gave written informed consent and enrolled in a protocol approved by the National Institute of Arthritis and Musculoskeletal and Skin Diseases (NIAMS) Institutional Review Board (IRB protocol 01-AR-0227, NIH-94-AR-0066), the University of Michigan IRB (IRB protocol HUM00043667 or HUM00045058), and the Instituto Nacional de Ciencias Medicas y

de la Nutricion Salvador Zubiran (INCMNSZ, Ref 1243). A complete clinical examination was performed, Disease Activity Score (DAS-28) was determined (*38*), and hand and foot radiographs scores were obtained using the Simple Erosion Narrowing Score (SENS) (*39*, *40*) for the RA samples provided by the Instituto Nacional de Ciencias Medicas y Nutricion Salvador Zubiran (cohort 2). The rheumatologist who scored the radiographs was blinded to the patients' clinical data. PB was obtained by venipuncture and collected in EDTA-containing tubes. PB was fractionated via Ficoll-Paque Plus (GE Healthcare) gradient. Neutrophils were isolated by dextran sedimentation and hypotonic salt solution as previously described (*10*).

RA FLS were obtained as previously described (*41*). Cells were maintained in CMRL medium (Invitrogen Life Technologies) and used after passage 4 from primary cultures. Macrophages were maintained in RPMI (Invitrogen Life Technologies), and OCs were cultured in α-MEM (Invitrogen Life Technologies). Cell cultures were supplemented with 10% FBS (Invitrogen), 2 mM glutamine, penicillin (100 U/ml), and streptomycin (100 μg/ml) and grown in a humidified incubator with 5% CO_2 at 37°C.

PB $CD14^+$ monocytes were isolated from healthy volunteers as previously described (*42*). Briefly, PB mononuclear cells (PBMCs) were incubated with CD14 beads (Miltenyi Biotec) in MACS buffer according to the manufacturer's instructions.

NET generation and carbamylation

Neutrophils from healthy volunteers were resuspended in RPMI and seeded in 24-well plates in the presence of PMA (100 ng/ml) in the presence or absence of 100 μM CN for 4 hours at 37°C. NETs were harvested with micrococcal nuclease (10 U/ml) (Thermo Fisher Scientific, Waltham, MD) for 15 min at 37°C. NETs were collected and cleared of debris by centrifugation and stored at −20°C.

Immunization of DRB1*04:01 mice with NETs and cNETs

Animal studies were performed according to the guidance established by the NIAMS Laboratory Animal Care and Use Section and following approved protocol (A016-05-26). Breeding pairs of DRB1*04:01 transgenic mice were a gift from C. David (Mayo Clinic), and they were housed and bred at the National Institutes of Health (NIH) animal facility. Twelve-week-old DRB1*04:01 male and female mice were anesthetized using isoflurane vaporization. Hind left leg was shaved and injected intra-articularly with 10 μl of total NETs, cNETs, or RA-NETs using a 27-gauge needle. This procedure was performed weekly for a total of 14 weeks. Serum was collected at weeks 6 and 14 and analyzed for the presence of ACPAs and anti-CarP antibodies.

Quantification of complexes of citrullinated histone H4–DNA and carbamylated-DNA by ELISA

Serum citrullinated histone H3 or citrullinated histone H4 or carbamylated protein–dsDNA (double-stranded DNA) complexes were quantified by ELISA. A 96-well plate was coated with rabbit polyclonal anti-citrullinated histone 3 (Abcam) or citrullinated histone 4 (EMD Millipore) or carbamylated lysine (Cell Biolabs) antibodies at 1:400 in phosphate-buffered saline (PBS) overnight at 4°C. Wells were washed and blocked with 1% bovine serum albumin (BSA) at room temperature for 1 hour. Diluted plasma (1:10) was added to the wells in (1% BSA) blocking buffer and incubated overnight at 4°C. The wells were washed three times and incubated with mouse monoclonal anti-dsDNA antibody (EMD Millipore) at 1:100 in blocking buffer. After washing three times, goat anti-mouse–conjugated horseradish peroxidase (HRP) antibody (Bio-Rad) was added to the wells in blocking buffer at 1:10,000. Wells were washed five times followed by the addition of tetramethylbenzidine (TMB) substrate (Sigma-Aldrich) and stop solution (Sigma-Aldrich). The absorbance was measured at 450 nm, and values were calculated as an optical density (OD) index. Assay was performed in duplicate.

cNET ELISA

A 96-well plate was coated with cNETs (4 μg/ml) in RPMI overnight at 4°C. Wells were washed and blocked with 1% BSA at room temperature for 1 hour. Diluted plasma (1:10) was added to the wells in (1% BSA) blocking buffer and incubated overnight at 4°C. The wells were washed three times, and donkey anti-human IgG–conjugated HRP antibody (Bio-Rad) was added to the wells in blocking buffer at 1:10,000. Wells were washed five times followed by the addition of TMB substrate (Sigma-Aldrich) and stop solution (Sigma-Aldrich). The absorbance was measured at 450 nm, and values were calculated as an OD index. Assay was performed in duplicate.

Proteomic analysis

Immunoprecipitated proteins were run on a 4 to 12% bis-tris gradient gel. After staining with Coomassie blue, the excised bands were destained, reduced, alkylated, and digested with trypsin as previously described (*43*). Desalted tryptic peptides were analyzed using nanoscale liquid chromatography tandem mass spectrometry (nLC-MS/MS) and Ultimate 3000-nLC online coupled with an Orbitrap Lumos Tribrid mass spectrometer (Thermo Fisher Scientific). Peptides were separated on an EASY-Spray C_{18} column (Thermo Fisher Scientific; 75 μm–by–50 cm inner diameter, 2-μm particle size, and 100-Å pore size). Separation was achieved by 4 to 28% linear gradient of acetonitrile + 0.1% formic acid for 65 min. An electrospray voltage of 1.9 kV was applied to the eluent via the EASY-Spray column electrode. The Orbitrap Lumos was operated in positive ion data-dependent mode. Full-scan MS^1 was performed in the Orbitrap with a normal precursor mass range of 375 to 1500 *m/z* (mass/charge ratio) at a resolution of 120,000. The automatic gain control (AGC) target and maximum accumulation time settings were set to 4×10^5 and 50 ms, respectively. MS^2 was triggered by selecting the most intense precursor ions above an intensity threshold of 2×10^4 for higher-energy collisional dissociation (HCD)–MS^2 fragmentation with an AGC target and maximum accumulation time settings of 2.5×10^4 and 125 ms, respectively. Mass filtering was performed by the quadrupole with 0.7 *m/z* transmission window, followed by HCD fragmentation in the Orbitrap and collision energy of 32% at a resolution of 30,000. To improve the spectral acquisition rate, parallelizable time was activated. The number of MS^2 spectra acquired between full scans was restricted to a duty cycle of 3 s. Raw data files were processed with the Proteome Discoverer software (v2.4, Thermo Fisher Scientific), using Byonic v3.3.3 (Protein Metrics) search node for carbamylated peptide/protein identifications. The following search parameters were set for MS1 tolerance of 10 parts per million (ppm): orbitrap-detected MS/MS mass tolerance of 0.02 Da; enzyme specificity set as trypsin with maximum three missed cleavages; minimum peptide length of 6 amino acids; fixed modification of Cys (carbamidomethylation); variable modification of methionine oxidation; carbamylation of N terminus and Lys; and deamidation of Arg (citrullination), Asn, and Gln. Target decoy was used to calculate the false discovery rate of peptide spectrum matches, set at $P < 0.02$ (*44*).

Furthermore, the b- and y-series ions of the carbamylated peptides were investigated individually for neutral loss of isocyanic acid (HNCO) −43.0058 Da.

ACPA depletion and purification

ACPAs were isolated by affinity purification, modified from protocols previously published. In brief, 13 μg of biotinylated-CCP2 (gift from Leiden University) was incubated with 50 ul of streptavidin-agarose slurry (Thermo Fisher Scientific) for 60 min at room temperature. CCP2-bound agarose beads were washed three times with cold PBS. Serum from patients with established RA from a long-standing prospective cohort (*45*) was diluted (1:500) with 1% BSA and incubated with CCP2-bound agarose beads overnight at 4C. ACPA-depleted sera were stored at −80°C until further use. Beads were washed twice with cold PBS, and ACPAs were eluted with low-pH elution buffer (Thermo Fisher Scientific). Solution was neutralized according to the manufacturer's instructions.

Autoantibody quantification by ELISA

A 96-well plate was coated with recombinant carbamylated histone H2A, histone H2B, histone H3, histone H4, α-enolase, or vimentin (100 ng/ml) in PBS overnight at 4°C. The plate was washed and blocked with 1% BSA for 1 hour at room temperature. Diluted (1:500) sera from SLE patients, RA patients, and healthy donors were incubated overnight at 4°C. The plate was washed three to five times with 0.05% PBS-Tween (PBS-T). HRP-conjugated anti-human IgG secondary antibody was incubated for 1 hour at room temperature, followed by five to seven washes with PBS-T. The plate was developed in the presence of TMB and read at 450 nm using a microplate reader (Synergy HT, BioTek). Results are presented as OD index (ratio of the OD in the patient serum to the mean OD in healthy control serum).

Cocultures of cells with NETs

A 12-well plate was seeded with 20,000 RA FLS or 20,000 M1 macrophages and treated with 100 μg of PMA-generated NETs or PMA + CN–generated NETs (cNETs) for 24 hours. RNA was isolated using a Direct-zol RNA Miniprep kit (Zymo Research) according to the manufacturer's instructions. Complementary DNA (cDNA) was synthesized using an iScript RT single-strand cDNA master mix (Bio-Rad). Fold difference was calculated using $\Delta\Delta C_t$ equation.

Effect of immune complexes on OC formation

A 96-well plate was coated with 200 ng of carbamylated histone H3/H4 in PBS overnight. Immune complexes were generated by adding 100 μg of total IgG isolated from RA serum using a Melon kit (Thermo Fisher Scientific). After 2 hours of incubation, wells were washed with PBS. $CD14^+$ cells were isolated from healthy control PBMCs using MACS columns with positive selection. Cells were incubated in the presence of M-CSF (50 ng/ml) for 3 days. These pre-OCs were seeded in the previously coated plates with carbamylated histone H3/H4 in the presence or absence of control or RA IgGs. Cells were maintained with M-CSF and RANKL. After 3 days, the plate was washed and a TRAP staining kit (company) was used to detect TRAP-positive cells.

OC resorption assay

$CD14^+$ cells were isolated from PBMCs from healthy control using MACS columns. Cells were incubated in the presence of M-CSF (50 ng/ml) for 3 days, followed by incubation with RANKL (100 ng/ml) for 7 days. OCs were detached using nonenzymatic dissociation solution (Sigma-Aldrich). Equal numbers of OCs were seeded in a calcium phosphate–coated plate in the presence or absence of carbamylated histone H3/H4, carbamylated histone H3/H4–control IgG, or carbamylated histone H3/H4–RA IgG. OCs were cultured in the presence of RANKL (100 ng/ml) for 3 days. Cells were removed, and the plate was washed and scanned in a Celigo instrument. Images were analyzed using ImageJ.

Immunofluorescence

Neutrophils were fixed in 4% paraformaldehyde (PFA) in PBS overnight at 4°C, washed, and blocked with 0.2% porcine gelatin (Sigma-Aldrich, St. Louis, MO) for 30 min and then incubated with primary antibody for 1 hour in a humid chamber at 37°C. Coverslips were then washed three times and incubated for 30 min with secondary antibody at 37°C. Nuclei were counterstained with 1:1000 Hoechst at room temperature. After washing three more times, coverslips were mounted on glass slides using ProLong Gold solution (Invitrogen). Images were acquired on a Zeiss LSM 780 confocal microscope.

Detection of citrullination using Rh-PG probe

Citrulline probe was used as previously described (*11*). Briefly, 10 μg of total NETs from carbamylated and non-carbamylated samples was incubated with 100 μM citrulline–Rh-PG probe (Cayman) in 20% trichloroacetic acid for 30 min at 37°C. Samples were washed with cold acetone twice and separated in a 4 to 12% gradient bis-tris gel (Invitrogen). Citrullinated proteins were visualized in an Azure c600 Imaging system (Azure Biosystems).

Western blotting

Equal amounts of NETs were resolved in a 4 to 12% gradient bis-tris gel (Invitrogen), transferred onto a nitrocellulose membrane, and blocked with 10% BSA for 30 min at room temperature. After overnight incubation with primary antibodies, membranes were washed three times with PBS-T and incubated with secondary antibody coupled to IRDye 800CW. Membranes were developed using Li-COR Odyssey Clx scanner (Li-COR).

Statistical analysis

All analyses were performed using GraphPad Prism version 8.1.1 (La Jolla, CA). Mann-Whitney *U* test was used as applicable. One-way analysis of variance (ANOVA) Kruskal-Wallis test (Dunn's multiple comparison test) was used to compare parameters among groups. All analyses were considered statistically significant at $P < 0.05$. A correlation matrix was generated in R using base R and plotted using the package ggcorplot (v0.1.3). Code is available upon request.

SUPPLEMENTARY MATERIALS

Supplementary material for this article is available at http://advances.sciencemag.org/cgi/content/full/6/44/eabd2688/DC1

View/request a protocol for this paper from *Bio-protocol*.

REFERENCES AND NOTES

1. V. M. Holers, Autoimmunity to citrullinated proteins and the initiation of rheumatoid arthritis. *Curr. Opin. Immunol.* **25**, 728–735 (2013).
2. B. A. Fisher, P. J. Venables, Inhibiting citrullination in rheumatoid arthritis: Taking fuel from the fire. *Arthritis Res. Ther.* **14**, 108 (2012).
3. M. Brink, M. Hansson, L. Mathsson, P.-J. Jakobsson, R. Holmdahl, G. Hallmans, H. Stenlund, J. Rönnelid, L. Klareskog, S. Rantapää-Dahlqvist, Multiplex analyses of antibodies against

citrullinated peptides in individuals prior to development of rheumatoid arthritis. *Arthritis Rheum.* **65**, 899–910 (2013).
4. W. P. Arend, G. S. Firestein, Pre-rheumatoid arthritis: Predisposition and transition to clinical synovitis. *Nat. Rev. Rheumatol.* **8**, 573–586 (2012).
5. J. Shi, R. Knevel, P. Suwannalai, M. P. van der Linden, G. M. Janssen, P. A. van Veelen, N. E. Levarht, A. H. van der Helm-van Mil, A. Cerami, T. W. Huizinga, R. E. Toes, L. A. Trouw, Autoantibodies recognizing carbamylated proteins are present in sera of patients with rheumatoid arthritis and predict joint damage. *Proc. Natl. Acad. Sci. U.S.A.* **108**, 17372–17377 (2011).
6. L. Vidal-Bralo, E. Perez-Pampin, C. Regueiro, A. Montes, R. Varela, M. D. Boveda, J. J. Gomez-Reino, A. Gonzalez, Anti-carbamylated protein autoantibodies associated with mortality in Spanish rheumatoid arthritis patients. *PLOS ONE* **12**, e0180144 (2017).
7. L. A. Trouw, T. Rispens, R. E. M. Toes, Beyond citrullination: Other post-translational protein modifications in rheumatoid arthritis. *Nat. Rev. Rheumatol.* **13**, 331–339 (2017).
8. S. Kalim, S. A. Karumanchi, R. I. Thadhani, A. H. Berg, Protein carbamylation in kidney disease: Pathogenesis and clinical implications. *Am. J. Kidney Dis.* **64**, 793–803 (2014).
9. C. Ospelt, H. Bang, E. Feist, G. Camici, S. Keller, J. Detert, A. Krämer, S. Gay, K. Ghannam, G. R. Burmester, Carbamylation of vimentin is inducible by smoking and represents an independent autoantigen in rheumatoid arthritis. *Ann. Rheum. Dis.* **76**, 1176–1183 (2017).
10. R. Khandpur, C. Carmona-Rivera, A. Vivekanandan-Giri, A. Gizinski, S. Yalavarthi, J. S. Knight, S. Friday, S. Li, R. M. Patel, V. Subramanian, P. Thompson, P. Chen, D. A. Fox, S. Pennathur, M. J. Kaplan, NETs are a source of citrullinated autoantigens and stimulate inflammatory responses in rheumatoid arthritis. *Sci. Transl. Med.* **5**, 178ra140 (2013).
11. C. Carmona-Rivera, P. M. Carlucci, E. Moore, N. Lingampalli, H. Uchtenhagen, E. James, Y. Liu, K. L. Bicker, H. Wahamaa, V. Hoffmann, A. I. Catrina, P. Thompson, J. H. Buckner, W. H. Robinson, D. A. Fox, M. J. Kaplan, Synovial fibroblast-neutrophil interactions promote pathogenic adaptive immunity in rheumatoid arthritis. *Sci. Immunol.* **2**, eaag3358 (2017).
12. L.-M. Mauracher, F. Posch, K. Martinod, E. Grilz, T. Däullary, L. Hell, C. Brostjan, C. Zielinski, C. Ay, D. D. Wagner, I. Pabinger, J. Thaler, Citrullinated histone H3, a biomarker of neutrophil extracellular trap formation, predicts the risk of venous thromboembolism in cancer patients. *J. Thromb. Haemost.* **16**, 508–518 (2018).
13. D. N. Douda, M. A. Khan, H. Grasemann, N. Palaniyar, SK3 channel and mitochondrial ROS mediate NADPH oxidase-independent NETosis induced by calcium influx. *Proc. Natl. Acad. Sci. U.S.A.* **112**, 2817–2822 (2015).
14. V. Brinkmann, U. Reichard, C. Goosmann, B. Fauler, Y. Uhlemann, D. S. Weiss, Y. Weinrauch, A. Zychlinsky, Neutrophil extracellular traps kill bacteria. *Science* **303**, 1532–1535 (2004).
15. E. A. Chapman, M. Lyon, D. Simpson, D. Mason, R. J. Beynon, R. J. Moots, H. L. Wright, Caught in a trap? Proteomic analysis of neutrophil extracellular traps in rheumatoid arthritis and systemic lupus erythematosus. *Front. Immunol.* **10**, 423 (2019).
16. S. A. Elsayed, M. A. Esmail, R. M. Ali, O. M. Mohafez, Diagnostic and prognostic value of anti-CarP antibodies in a sample of Egyptian rheumatoid arthritis patients. *Clin. Rheumatol.* **38**, 2683–2689 (2019).
17. H. Koppejan, L. A. Trouw, J. Sokolove, L. J. Lahey, T. J. W. Huizinga, I. A. Smolik, D. B. Robinson, H. S. El-Gabalawy, R. E. Toes, C. A. Hitchon, Role of anti–carbamylated protein antibodies compared to anti–citrullinated protein antibodies in indigenous north americans with rheumatoid arthritis, their first-degree relatives, and healthy controls. *Arthritis Rheumatol.* **68**, 2090–2098 (2016).
18. S. Pan, T. Trejo, J. Hansen, M. Smart, C. S. David, HLA-DR4 (DRB1*0401) transgenic mice expressing an altered CD4-binding site: Specificity and magnitude of DR4-restricted T cell response. *J. Immunol.* **161**, 2925–2929 (1998).
19. P. K. Gregersen, J. Silver, R. J. Winchester, The shared epitope hypothesis. An approach to understanding the molecular genetics of susceptibility to rheumatoid arthritis. *Arthritis Rheum.* **30**, 1205–1213 (1987).
20. V. Taneja, M. Behrens, A. Mangalam, M. M. Griffiths, H. S. Luthra, C. S. David, New humanized HLA–DR4-transgenic mice that mimic the sex bias of rheumatoid arthritis. *Arthritis Rheum.* **56**, 69–78 (2007).
21. I. A. Udalova, A. Mantovani, M. Feldmann, Macrophage heterogeneity in the context of rheumatoid arthritis. *Nat. Rev. Rheumatol.* **12**, 472–485 (2016).
22. D. Abdallah, M.-L. Jourdain, J. Braux, C. Guillaume, S. C. Gangloff, J. Jacquot, F. Velard, An optimized method to generate human active osteoclasts from peripheral blood monocytes. *Front. Immunol.* **9**, 632 (2018).
23. Y. Tanaka, Clinical immunity in bone and joints. *J. Bone Miner. Metab.* **37**, 2–8 (2019).
24. S. Kumar, G. Pangtey, R. Gupta, H. S. Rehan, L. K. Gupta, Assessment of anti-CarP antibodies, disease activity and quality of life in rheumatoid arthritis patients on conventional and biological disease-modifying antirheumatic drugs. *Reumatologia* **55**, 4–9 (2017).
25. I. B. McInnes, G. Schett, The pathogenesis of rheumatoid arthritis. *N. Engl. J. Med.* **365**, 2205–2219 (2011).
26. I. B. McInnes, G. Schett, Cytokines in the pathogenesis of rheumatoid arthritis. *Nat. Rev. Immunol.* **7**, 429–442 (2007).
27. U. Harre, D. Georgess, H. Bang, A. Bozec, R. Axmann, E. Ossipova, P.-J. Jakobsson, W. Baum, F. Nimmerjahn, E. Szarka, G. Sarmay, G. Krumbholz, E. Neumann, R. Toes, H.-U. Scherer, A. I. Catrina, L. Klareskog, P. Jurdic, G. Schett, Induction of osteoclastogenesis and bone loss by human autoantibodies against citrullinated vimentin. *J. Clin. Invest.* **122**, 1791–1802 (2012).
28. B. Hauser, S. Zhao, M. R. Visconti, P. L. Riches, W. D. Fraser, I. Piec, N. J. Goodson, S. H. Ralston, Autoantibodies to osteoprotegerin are associated with low hip bone mineral density and history of fractures in axial spondyloarthritis: A cross-sectional observational study. *Calcif. Tissue Int.* **101**, 375–383 (2017).
29. C. Regueiro, A. M. Ortiz, M. D. Boveda, S. Castañeda, I. Gonzalez-Alvaro, A. Gonzalez, Association of high titers of anti-carbamylated protein antibodies with decreased bone mineral density in early arthritis patients. *PLOS ONE* **13**, e0202583 (2018).
30. S. Monti, C. Montecucco, S. Bugatti, R. Caporali, Rheumatoid arthritis treatment: The earlier the better to prevent joint damage. *RMD Open* **1**, e000057 (2015).
31. L. G. Schipper, M. Vermeer, H. H. Kuper, M. O. Hoekstra, C. J. Haagsma, A. A. Den Broeder, P. van Riel, J. Fransen, M. A. van de Laar, A tight control treatment strategy aiming for remission in early rheumatoid arthritis is more effective than usual care treatment in daily clinical practice: A study of two cohorts in the Dutch Rheumatoid Arthritis Monitoring registry. *Ann. Rheum. Dis.* **71**, 845–850 (2012).
32. A. K. Hedström, L. Klareskog, L. Alfredsson, Exposure to passive smoking and rheumatoid arthritis risk: Results from the Swedish EIRA study. *Ann. Rheum. Dis.* **77**, 970–972 (2018).
33. D. Makrygiannakis, M. Hermansson, A.-K. Ulfgren, A. P. Nicholas, A. J. Zendman, A. Eklund, J. Grunewald, C. M. Skold, L. Klareskog, A. I. Catrina, Smoking increases peptidylarginine deiminase 2 enzyme expression in human lungs and increases citrullination in BAL cells. *Ann. Rheum. Dis.* **67**, 1488–1492 (2008).
34. A. D. Joshi, M. G. Mustafa, C. F. Lichti, C. J. Elferink, Homocitrullination is a novel histone h1 epigenetic mark dependent on aryl hydrocarbon receptor recruitment of carbamoyl phosphate synthase 1. *J. Biol. Chem.* **290**, 27767–27778 (2015).
35. S. W. Scally, J. Petersen, S. C. Law, N. L. Dudek, H. J. Nel, K. L. Loh, L. C. Wijeyewickrema, S. B. Eckle, J. van Heemst, R. N. Pike, J. McCluskey, R. E. Toes, N. L. La Gruta, A. W. Purcell, H. H. Reid, R. Thomas, J. Rossjohn, A molecular basis for the association of the *HLA-DRB1* locus, citrullination, and rheumatoid arthritis. *J. Exp. Med.* **210**, 2569–2582 (2013).
36. E. Villeneuve, J. Nam, P. Emery, 2010 ACR-EULAR classification criteria for rheumatoid arthritis. *Rev. Bras. Reumatol.* **50**, 481–483 (2010).
37. E. M. Tan, A. S. Cohen, J. F. Fries, A. T. Masi, D. J. McShane, N. F. Rothfield, J. G. Schaller, N. Talal, R. J. Winchester, The 1982 revised criteria for the classification of systemic lupus erythematosus. *Arthritis Rheum.* **25**, 1271–1277 (1982).
38. M. L. Prevoo, M. A. van't Hof, H. H. Kuper, M. A. van Leeuwen, L. B. van de Putte, P. L. van Riel, Modified disease activity scores that include twenty-eight-joint counts. Development and validation in a prospective longitudinal study of patients with rheumatoid arthritis. *Arthritis Rheum.* **38**, 44–48 (1995).
39. E. M. Dias, C. Lukas, R. Landewé, S. Fatenejad, D. van der Heijde, Reliability and sensitivity to change of the Simple Erosion Narrowing Score compared with the Sharp-van der Heijde method for scoring radiographs in rheumatoid arthritis. *Ann. Rheum. Dis.* **67**, 375–379 (2008).
40. D. van der Heijde, T. Dankert, F. Nieman, R. Rau, M. Boers, Reliability and sensitivity to change of a simplification of the Sharp/van der Heijde radiological assessment in rheumatoid arthritis. *Rheumatology* **38**, 941–947 (1999).
41. C. N. Tran, M. J. Davis, L. A. Tesmer, J. L. Endres, C. D. Motyl, C. Smuda, E. C. Somers, K. C. Chung, A. G. Urquhart, S. K. Lundy, S. Kovats, D. A. Fox, Presentation of arthritogenic peptide to antigen-specific T cells by fibroblast-like synoviocytes. *Arthritis Rheum.* **56**, 1497–1506 (2007).
42. C. Carmona-Rivera, S. S. Khaznadar, K. W. Shwin, J. A. Irizarry-Caro, L. J. O'Neil, Y. Liu, K. A. Jacobson, A. K. Ombrello, D. L. Stone, W. L. Tsai, D. L. Kastner, I. Aksentijevich, M. J. Kaplan, P. C. Grayson, Deficiency of adenosine deaminase 2 triggers adenosine-mediated NETosis and TNF production in patients with DADA2. *Blood* **134**, 395–406 (2019).
43. C. M. Van Itallie, A. J. Tietgens, K. LoGrande, A. Aponte, M. Gucek, J. M. Anderson, Phosphorylation of claudin-2 on serine 208 promotes membrane retention and reduces trafficking to lysosomes. *J. Cell Sci.* **125**, 4902–4912 (2012).
44. J. E. Elias, S. P. Gygi, Target-decoy search strategy for mass spectrometry-based proteomics. *Methods Mol. Biol.* **604**, 55–71 (2010).
45. S. Tanner, B. Dufault, I. Smolik, X. Meng, V. Anaparti, C. Hitchon, D. B. Robinson, W. Robinson, J. Sokolove, L. Lahey, E. D. Ferucci, H. El-Gabalawy, A prospective study of the development of inflammatory arthritis in the family members of indigenous

North American people with rheumatoid arthritis. *Arthritis Rheumatol.* **71**, 1494–1503 (2019).

Acknowledgments
Funding: This study was supported by the Intramural Research Program, NIAMS/NIH, ZIA AR041199. **Author contributions:** L.J.O., D.S.-H., and C.C.-R. performed the experiments. L.J.O., A.B.-V., J.M.-C., E.A.-A., and C.C.-R. analyzed the data and performed statistical analyses. A.M.A. and M.G. performed proteomic analyses. A.B.-V., J.M.-C., E.A.-A., Y.R.-P., D.A.F., J.D.K., and H.E.-G. provided specimens and clinical information. L.J.O., M.J.K., and C.C.-R. were involved in overall design and/or manuscript preparation. L.J.O., A.B.-V., M.J.K., and C.C.-R. drafted the manuscript. **Competing interests:** The authors declare that they have no competing interests. **Data and materials availability:** All data needed to evaluate the conclusions in the paper are present in the paper and/or the Supplementary Materials. Additional data related to this paper may be requested from the authors.

Submitted 10 June 2020
Accepted 11 September 2020
Published 28 October 2020
10.1126/sciadv.abd2688

Citation: L. J. O'Neil, A. Barrera-Vargas, D. Sandoval-Heglund, J. Merayo-Chalico, E. Aguirre-Aguilar, A. M. Aponte, Y. Ruiz-Perdomo, M. Gucek, H. El-Gabalawy, D. A. Fox, J. D. Katz, M. J. Kaplan, C. Carmona-Rivera, Neutrophil-mediated carbamylation promotes articular damage in rheumatoid arthritis. *Sci. Adv.* **6**, eabd2688 (2020).

Neutrophil-mediated carbamylation promotes articular damage in rheumatoid arthritis

Liam J. O'Neil, Ana Barrera-Vargas, Donavon Sandoval-Heglund, Javier Merayo-Chalico, Eduardo Aguirre-Aguilar, Angel M. Aponte, Yanira Ruiz-Perdomo, Marjan Gucek, Hani El-Gabalawy, David A. Fox, James D. Katz, Mariana J. Kaplan and Carmelo Carmona-Rivera

Sci Adv **6** (44), eabd2688.
DOI: 10.1126/sciadv.abd2688